crystals

MDPI

Article

$La_{1-y}Ba_yF_{3-y}$ Solid Solution Crystals as an Effective Solid Electrolyte: Growth and Properties

Irina I. Buchinskaya, Denis N. Karimov * and Nikolay I. Sorokin

Shubnikov Institute of Crystallography of Federal Scientific Research Center «Crystallography and Photonics», Russian Academy of Sciences, Leninsky Prospekt 59, 119333 Moscow, Russia; buchinskayaii@gmail.com (I.I.B.); nsorokin1@yandex.ru (N.I.S.)

* Correspondence: dnkarimov@gmail.com; Tel.: +7-903-778-74-89

Abstract: A series of nonstoichiometric $La_{1-y}Ba_yF_{3-y}$ ($0 \leq y \leq 0.12$) single crystals with a tysonite-type structure (sp. gr. *P*-3*c*1) was grown from the melt by the directional crystallization method in a fluorinating atmosphere, and some physical properties were characterized. The concentration dependence of electrical conductivity $\sigma_{dc}(y)$ $La_{1-y}Ba_yF_{3-y}$ crystals was studied. The composition of the ionic conductivity maximum for this solid electrolyte was refined. It was confirmed that the maximum conductivity $\sigma_{max} = 8.5 \times 10^{-5}$ S/cm (295 K) was observed at the composition $y_{max} = 0.05 \pm 0.01$. Analysis of the electrophysical data for the group of tysonite-type solid electrolytes $R_{1-y}M_yF_{3-y}$ (M = Ca, Sr, Ba, Eu^{2+} and R = La, Ce, Pr, Nd) showed that the compositions of the maxima of their conductivity were close and amount to $y = 0.03-0.05$. This fact indicates a weak influence of the size effect (ionic radii R^{3+} and M^{2+}) on the value of y_{max} for $R_{1-y}M_yF_{3-y}$ solid electrolytes.

Keywords: complex fluoride; solid solutions; $La_{1-y}Ba_yF_{3-y}$; growth from the melt; bulk crystals; Bridgman technique; rare-earth ions; ionic conductivity; optical materials; tysonite structure

check for updates

Citation: Buchinskaya, I.I.; Karimov, D.N.; Sorokin, N.I. $La_{1-y}Ba_yF_{3-y}$ Solid Solution Crystals as an Effective Solid Electrolyte: Growth and Properties. *Crystals* **2021**, *11*, 629. https://doi.org/10.3390/cryst11060629

Academic Editors: Xiang-Hua Zhang, Nataliya E. Novikova and Irina I. Buchinskaya

Received: 13 May 2021
Accepted: 29 May 2021
Published: 31 May 2021

Publisher's Note: MDPI stays neutral with regard to jurisdictional claims in published maps and institutional affiliations.

Copyright: © 2021 by the authors. Licensee MDPI, Basel, Switzerland. This article is an open access article distributed under the terms and conditions of the Creative Commons Attribution (CC BY) license (https://creativecommons.org/licenses/by/4.0/).

1. Introduction

One of the paths in the search for new materials with specified properties in modern materials science is the complication of chemical composition, i.e., transition from one-component to multicomponent crystals. Nonstoichiometric phases $M_{1-x}R_xF_{2+x}$ with a fluorite-type structure and $R_{1-y}M_yF_{3-y}$ with tysonite-type one are formed in all binary systems MF_2–RF_3 (M are alkaline-earth elements; R are rare-earth elements). With a change in the component concentration of such phases, the physical properties of crystals vary in wide ranges due to heterovalent isomorphic substitutions. The ability to smoothly change the chemical composition of crystals allows effectively controlling the physical properties and determining compositions with an optimal combination of parameters.

Wide areas of solid solutions with a fluorite-type (sp. gr. *Fm*-3*m*) structure $Ba_{1-x}La_xF_{2+x}$ ($0 \leq x \leq 0.52$) and with a tysonite-type (sp. gr. *P*-3*c*1) structure $La_{1-y}Ba_yF_{3-y}$ ($0 \leq y \leq 0.14$) are formed in a condensed system BaF_2–LaF_3 (Figure 1) [1]. These solid solutions demonstrate high stability to degradation; therefore, there is a possibility of growing both fluorite and tysonite single crystals from a melt in a wide concentration range. Heterovalent solid solutions $Ba_{1-x}La_xF_{2+x}$ [2] and $La_{1-y}Ba_yF_{3-y}$ are promising optical materials with variable properties due to the changeable composition. Their high fluorine-ionic conductivity σ_{dc} is especially attractive. [3–7]. They have very low electronic conductivity [8,9] and therefore are effective fluorine-conducting solid electrolytes. The method of growing fluorite-type crystals $Ba_{1-x}La_xF_{2+x}$ is well developed, and their electrophysical properties have been studied in detail [3–7,10,11]. Tysonite $La_{1-y}Ba_yF_{3-y}$ crystals have higher conductometric characteristics than $Ba_{1-x}La_xF_{2+x}$, but the conditions for their preparation and properties have been studied much less. At the present time, the solid electrolyte $La_{1-y}Ba_yF_{3-y}$ in terms of the set of performance characteristics has been proposed for use in the designs of the prototypes of fluorine-ion current sources of a new generation [12–16].

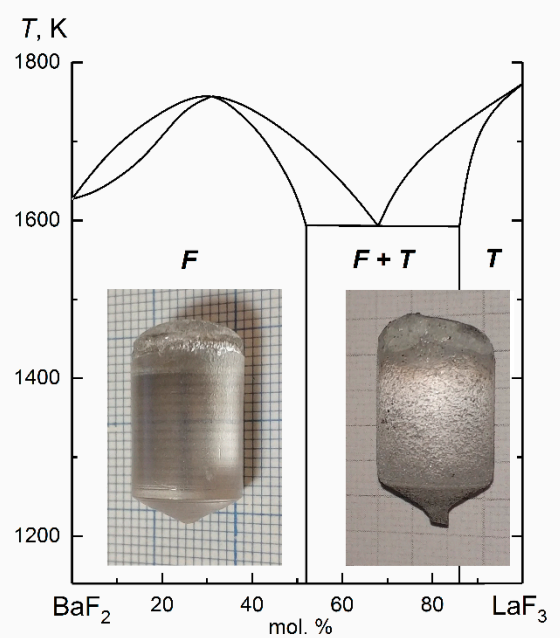

Figure 1. Phase diagram of the BaF_2–LaF_3 system [1] and the appearance of the grown crystals of the $La_{0.93}Ba_{0.07}F_{2.93}$ tysonite (***T***) phase. As an example, the previously grown single crystal of the fluorite (***F***) phase $Ba_{0.69}La_{0.31}F_{2.31}$ [2] is shown for comparison.

Bulk $R_{1-y}M_yF_{3-y}$ (R = La–Lu, Y, and M = Ca, Sr, Ba) crystals are usually grown by melt crystallization methods, predominantly the Bridgman–Stockbarger method [17,18] or Czochralski method. [19,20]. The Bridgman–Stockbarger method is technologically simple and allows, due to the use of multi-cell crucibles, a concentration series of solid solution crystals to grow under identical preparative and thermal conditions.

The ionic conductivity σ_{dc} of $La_{1-y}Ba_yF_{3-y}$ solid electrolyte was studied on polycrystalline samples [21–24], single crystals [5], nanoceramics [24–29], and films [30,31]. It was found that the concentration dependence $\sigma_{dc}(y)$ has a nonmonotonic character and passes through a maximum σ_{max} at the composition $y = y_{max}$. The conductivity values significantly depend on the technological form (crystals, ceramics, films, etc.) of the material and are maximum for single crystals.

Bulk single crystals are of particular interest for studying the fundamental characteristics of ionic transfer since only the single-crystal form gives fundamental conductivity values that are not distorted by the influence of the grain boundaries and pores. Investigating single crystals can accurately identify the composition $La_{1-y}Ba_yF_{3-y}$ solid solution, which corresponds to the maximum conductivity level. It is known that electrophysical studies of $La_{1-y}Ba_yF_{3-y}$ single crystals were carried out in [5] only. The authors used samples with a large step in composition y, which made it impossible to determine the coordinate of the σ_{max} exactly. A large scatter in the experimental data on the value y_{max} = 0.04–0.06 [21,24,28], 0.07–0.09 [5,22], 0.10 [25,27,30], and 0.15 [26] was observed for $La_{1-y}Ba_yF_{3-y}$ solid solution crystals.

Until now, there are few studies on growing concentrated tysonite-type fluoride solid solutions. Only the possibility of growing crystals of $R_{1-y}Sr_yF_{3-y}$ (R = La–Nd ($0 \leq y \leq 0.16$)) tysonite solid solutions, which are isostructural to $La_{1-y}Ba_yF_{3-y}$ crystals, have been studied [17,32]. These SrF_2-containing solid solutions have an important advantage for crystallization from a melt–congruent compositions corresponding to a singular point (temperature maximum) on the liquidus curve. The crystals with a homogeneous axial and radial distribution of the components can be grown in the vicinity of this chemical composition. Unfortunately, $La_{1-y}Ba_yF_{3-y}$ solid solution does not have compositions with congruent melting; a large difference in the liquidus and solidus temperatures leads to a significant

inhomogeneous distribution of the components along the length of the crystals during directional crystallization from the melt.

The aims of the present work are:

—Growing from the melt of concentration series of $La_{1-y}Ba_yF_{3-y}$ single crystals under identical conditions and its some physical properties characterization;

—Measurement of their ionic conductivity to refine y_{max} on the dependence $\sigma_{dc}(y)$;

—Comparative analysis of conductometric data for tysonite-type solid electrolytes in systems MF_2–RF_3 with M = Ca, Sr, Ba, Pb, Eu^{2+} and R = La, Ce, Pr, Nd.

2. Materials and Methods

2.1. The Peculiarities of the Growth Process

On the one hand, the proximity of the melting temperatures of LaF_3 (T_{fus} = 1773 ± 10 K) and BaF_2 (T_{fus} = 1627 ± 5 K) and their low volatility contribute to the production of $La_{1-y}Ba_yF_{3-y}$ single crystals from the melt by the direction crystallization method; on the other hand, this is hindered by the incongruent melting of the solid solution, as mentioned earlier. For tysonite-type structure, solid solutions, in comparison with fluorite-type structure solutions, a tendency to melt supercooling and spontaneous nucleation are characteristic [11], which prevents the growth of the high-quality bulk crystals. These problems are solved by increasing the temperature gradient at the growth interface and reducing the crucible pulling rate [10].

The $La_{1-y}Ba_yF_{3-y}$ solid solution compositions were chosen in the range $0 \leq y \leq 0.12$ for the investigation. The crystals were grown by the vertical directional crystallization method in a two-section growth facility with resistive heating in graphite crucibles using non-oriented seeds. BaF_2 (purity 99.99%, Sigma-Aldrich, Darmstadt, Germany) and LaF_3 (99.99%, Lanhit Ltd., Moscow, Russia) powders were used as starting reagents. The initial powders were preliminarily calcined in a vacuum (~10^{-2} Pa) at a temperature of 450 K and remelted to remove oxygen-containing impurities. The temperature gradient in the growth zone was ~100 K/cm and the crucible pulling rate was 3 mm/h. It should be noted that 5 wt.% PbF_2 was added to the charge as an oxygen scavenger in [32,33]. This is not the best choice because PbF_2 is not completely removed from the RF_3 and MF_2 melts and obviously modifies the physical properties of the crystals. Probably, at low concentrations of PbF_2 in some systems, azeotropic mixtures are formed [33,34]. Therefore, in our work, a mixture of high-purity He + CF_4 was used to create a fluorinating atmosphere in growth experiments. The evaporation loss during crystallization was no more than 2 wt. %. The $La_{1-y}Ba_yF_{3-y}$ tysonite-type crystals with a diameter of 12–14 mm and a length of up to 30 mm with the compositions y = 0; 0.005; 0.025; 0.035; 0.050; 0.060; 0.080; 0.090; 0.100; 0.120 (by charge) were successfully grown. The $Ba_{1-x}La_xF_{2+x}$ fluorite-type crystals in the range $0 \leq x \leq 0.50$ and eutectic composite (BaF_2/LaF_3 = 0.68/0.32 by charge) were obtained by the above method for comparative analysis of properties.

Crystal samples were cut perpendicular to the growth axis from the ingots in the form of plane–parallel disks and were optically polished.

2.2. Density Measurement

The density $\rho(y)$ of the samples was measured by the hydrostatic method in distilled water at room temperature. The density measurement error was $\Delta\rho = \pm 5 \times 10^{-3}$ g/cm^3.

2.3. Refractive Indices

Refractive indices n_D for $La_{1-y}Ba_yF_{3-y}$ single crystals were measured using the refractometric technique with an accuracy of $\pm 5 \times 10^{-4}$. The light source was Na-lamp (λ = 0.589 μm).

2.4. X-ray Diffraction (XRD) Analysis

The XRD analysis of the crystals was carried out by X-ray powder diffractometer Rigaku MiniFlex 600 (CuKα radiation). The diffraction peaks were recorded within the

angle range 2θ from 10 to 140°. The calculation of the unit cell parameters $a(y)$ and $c(y)$ for sp. gr. *P*-3*c*1 was carried out by full-profile Rietveld analysis using the HighScore Plus software (PANanalytical, Almelo, The Netherlands).

Since a concentration gradient of the components along the crystals' length was observed, the chemical composition of each sample was refined in terms of the unit cell parameters according to the equations for the concentration dependence of the unit cell parameters [11] and density [35] for the $La_{1-y}Ba_yF_{3-y}$ solid solution.

2.5. The Electrical Conductivity Measurements

The static electrical conductivity σ_{dc} at a direct current of the $La_{1-y}Ba_yF_{3-y}$ crystals was determined by impedance spectroscopy [36]. The impedance measurements were carried out in the frequency range of 5 to 5 × 10^5 Hz using a Tesla B-507 impedance tester at temperatures of 294–800 K in a vacuum ~1 Pa. The relative measurement error did not exceed 5%.

3. Results and Discussion

3.1. Crystal Characterization

The grown $La_{1-y}Ba_yF_{3-y}$ crystalline boules were transparent and did not have cracks and light-scattering inclusions. The $La_{0.93}Ba_{0.07}F_{2.93}$ crystal is shown in Figure 1 as a typical sample.

According to XRD analysis, the $La_{1-y}Ba_yF_{3-y}$ samples were a single-phase solid solution and belonged to the tysonite (sp. gr. *P*-3*c*1) structural type (Figure 2a). The presence of impurity phases was not detected.

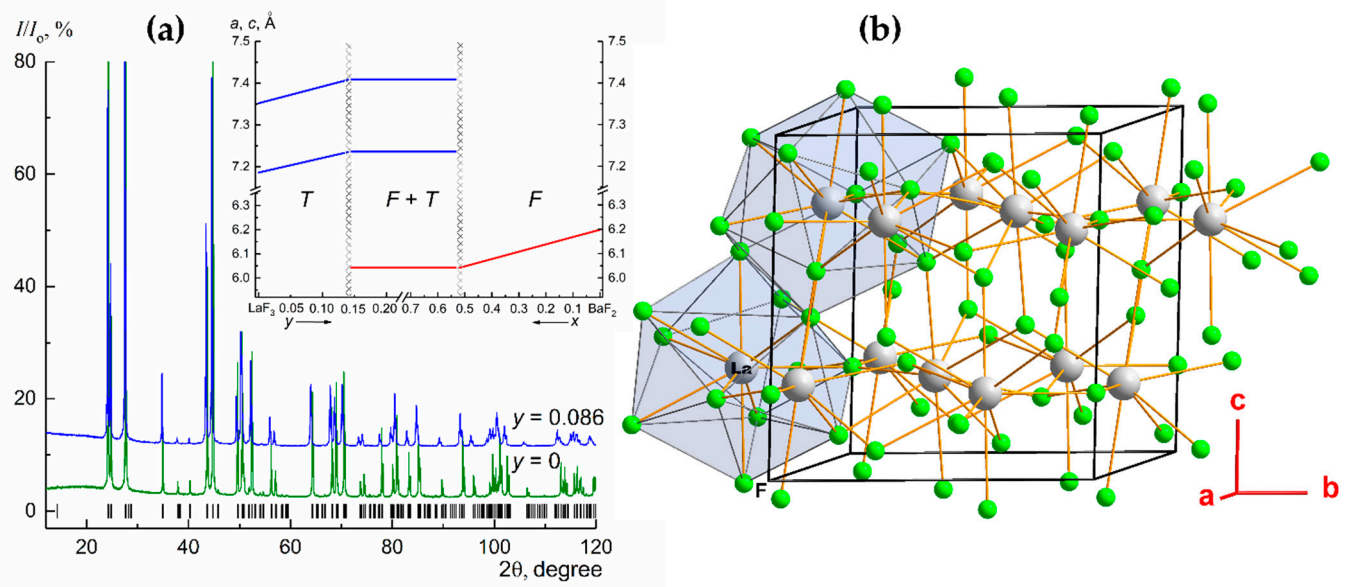

Figure 2. XRD patterns of $La_{1-y}Ba_yF_{3-y}$ crystal for selected y fraction (**a**). The positions of the Bragg reflections are indicated for sp. gr. *P*-3*c*1 with unit cell parameters a = 7.1832(1), c = 7.3493(1) Å. Inset: concentration dependence of the lattice parameters of the $La_{1-y}Ba_yF_{3-y}$ and $Ba_{1-x}La_xF_{2+x}$ solid solutions [11]. The data for the $Ba_{1-x}La_xF_{2+x}$ solid solution are presented for comparison. A perspective view of the LaF_3 tysonite crystal structure. Polyhedra for the La^{3+} cations are presented (**b**).

The unit cell parameters of this solid solution increase linearly with increasing of the fraction from y = 0 (a = 7.1832(1), c = 7.3493(1) Å) to limiting composition y = 0.14 (a = 7.2430(4), c = 7.4255(4) Å). An antibate dependence $a(x)$ was observed for the $Ba_{1-x}La_xF_{2+x}$ solid solution, the lattice parameter decreased from a = 6.1992(1) Å for x = 0 (pure BaF_2) to a = 6.0378(2) Å for the limiting composition x = 0.50. The observed concentration depen-

dences (Figure 2a, insert) coincided with the data of [1,11]. Eutectic composite contained both the saturated solid solution ($F + T$) which crystallized from the melt simultaneously.

The low-temperature tysonite modification is described in sp. gr. $P\text{-}3c1$ [37]. Purely anionic and cation-anionic layers alternated in the trigonal motif along the c axis (Figure 2b). The F^- anions were located in three non-equivalent structure positions. Substitution of La^{3+} cations on heterovalent M^{2+} ones led to the formation of vacancies in the fluorine sublattice (to maintain electroneutrality) and significantly affected the magnitude of the ionic conductivity of such tysonite solid solutions (see Section 3.2).

The $La_{1-y}Ba_yF_{3-y}$ crystals studied were uniaxial, optically negative, and were characterized by two refractive indices. The ordinary refractive index n_o was measured for $La_{1-y}Ba_yF_{3-y}$ crystals. The refractive index n_o ($\lambda = 0.589$ μm) of $La_{1-y}Ba_yF_{3-y}$ crystals decreased in a weakly square dependence from 1.5982(5) to 1.5841(5) with an increase in the fraction of y from 0 to 0.12 (Figure 3a). These crystals were highly refractive, exceeding the refractive indices of $Ba_{1-x}La_xF_{2+x}$ and other crystals with a fluorite-type structure. The known data for some other tysonite-type $R_{1-y}M_yF_{3-y}$ crystals are shown for comparison. The $La_{1-y}Ba_yF_{3-y}$ crystals were similar in refractive properties to other isostructural $La_{1-y}M_yF_{3-y}$ crystals (M = Ca, Sr, Ba) [17].

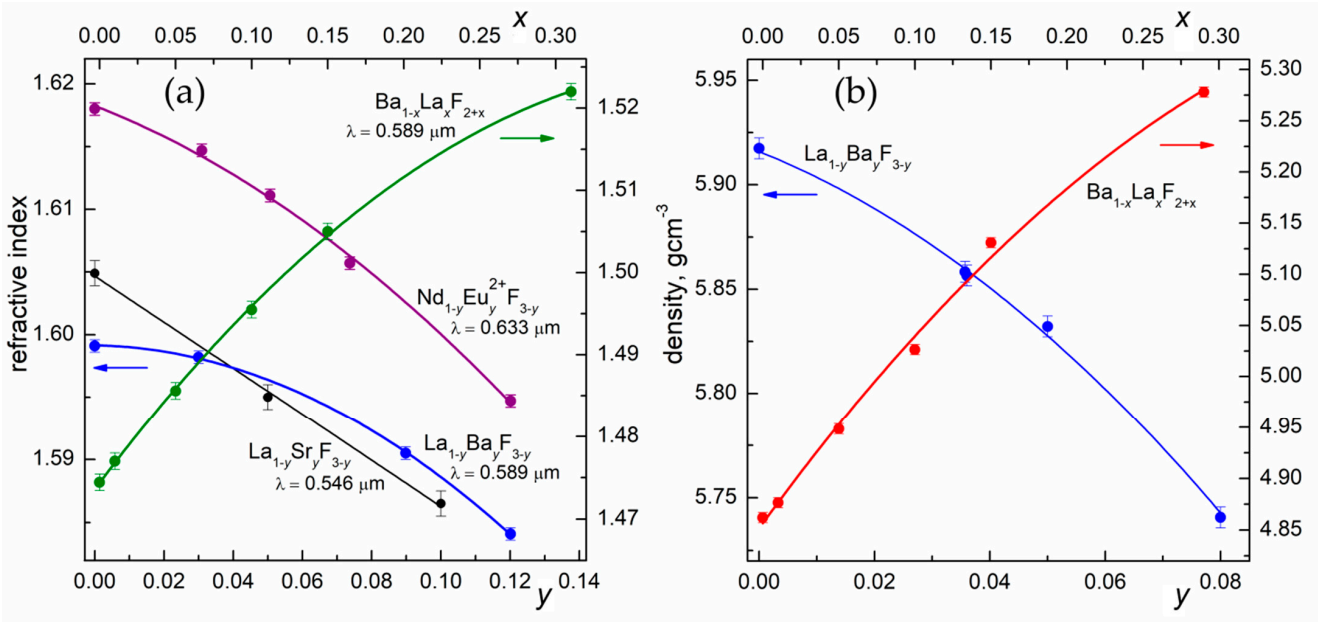

Figure 3. The concentration dependencies of the refractive indices (**a**) and densities (**b**) of the $La_{1-y}Ba_yF_{3-y}$ and some selected tysonite-type crystals. The data for the fluorite $Ba_{1-x}La_xF_{2+x}$ solid solution are presented for comparison.

The density of $La_{1-y}Ba_yF_{3-y}$ samples quadratically decreased in the range from 5.917(5) to 5.741(5) g/cm^3 with an increase in the fraction of y from 0 to 0.08 (Figure 3b) and exceeded the density of fluorite-type $Ba_{1-x}La_xF_{2+x}$ single crystals.

3.2. Ionic Conductivity of $La_{1-y}Ba_yF_{3-y}$ Crystals

We analyzed the impedance spectra of the $La_{1-y}Ba_yF_{3-y}$ crystals with silver electrodes. The impedance spectra were characterized by a depressed semi-circular arc at high frequency and an oblique tail at low frequency. As an example, Figure 4 shows the hodograph of the impedance $Z^*(\omega)$ for the $La_{0.994}Ba_{0.006}F_{2.994}$ crystal with Ag-electrodes. The impedance spectrum $Z^*(\omega)$ contained a semicircle (the center of which was displaced from the abscissa axis) simulating the electrical response from the crystal bulk and an oblique straight line (at low frequencies) simulating the electrical response from the crystal/electrode interface. An equivalent electrical circuit was used to describe the impedance hodographs. The circuit contained the crystal bulk resistivity R_b, the geometric capaci-

tance of the crystal C_g, and the capacitance of the double layer of the crystal/electrode interface C_{dl}.

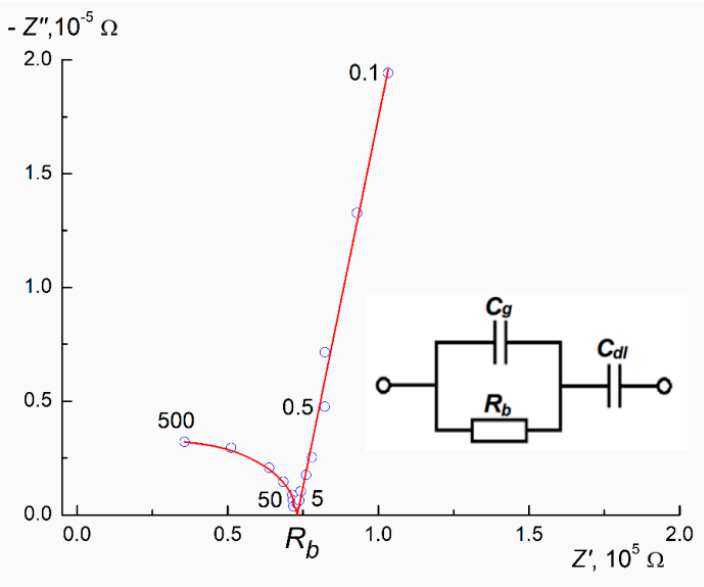

Figure 4. Impedance hodograph $Z^*(\omega)$ at 295 K for electrochemical cell Ag | $La_{0.994}Ba_{0.006}F_{2.994}$ | Ag and equivalent electrical circuit (insert). The frequency values in Hz are indicated.

The bulk resistance R_b was found from the intersection of the hodograph $Z^*(\omega)$ with the abscissa axis. Specific static electrical conductivity σ_{dc} was calculated by the formula:

$$\sigma_{dc} = {R_b}^{-1} h/S,$$

where h—sample thickness and S—electrode area. The temperature dependences of the ionic conductivity for $La_{1-y}Ba_yF_{3-y}$ crystals with y = 0.036 and 0.050 are shown in Figure 5a.

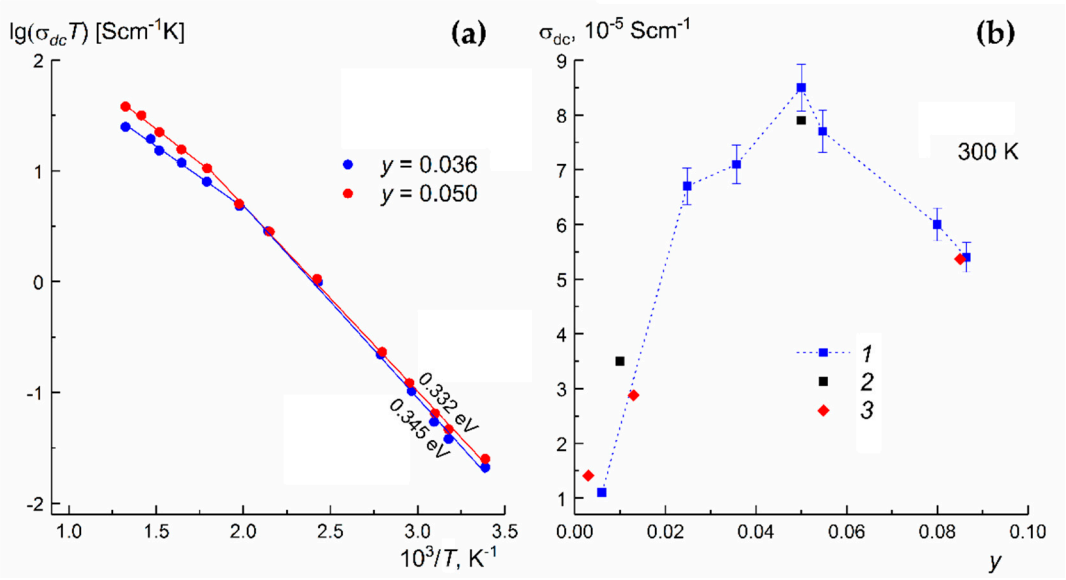

Figure 5. The temperature dependencies on ionic conductivity for the $La_{1-y}Ba_yF_{3-y}$ crystals. Solid lines represent fit according to an Arrhenius equation. The activation energies ΔH_σ are indicated (**a**). Concentration dependence of ionic conductivity $\sigma_{dc}(y)$ for $La_{1-y}Ba_yF_{3-y}$ solid electrolytes: *1*—this work, *2*—[38], *3*—[5] (**b**).

The $\sigma_{dc}(T)$ dependences for all studied samples were divided into two sections, which satisfy the Arrhenius-Frenkel equation:

$$\sigma_{dc}T = A\exp(-\Delta H_{\sigma}/k_{B}T),$$

where A—preexponential conductivity factor, ΔH_{σ}—activation enthalpy of ion transport, k_B—Boltzmann's constant, T—temperature. The Arrhenius—Frenkel equations parameters A and ΔH_{σ} are given in Table 1.

Table 1. Unit cell parameters a and c, preexponential conductivity factor A and activation enthalpy of ionic conductivity ΔH_{σ} for single crystals of $La_{1-y}Ba_yF_{3-y}$ solid electrolyte.

y	a, Å	c, Å	ΔT, K	A, SK/cm	ΔH_{σ}, eV
0.006 (1)	7.1882 (1)	7.3545 (1)	294–437 437–615	7.8×10^3 3.5×10^2	0.373 0.256
0.025 (1)	7.1947 (1)	7.3611 (1)	295–419 419–534	1.9×10^4 1.6×10^3	0.347 0.258
0.036 (2)	7.1985 (2)	7.3647 (1)	295–505 505–800	1.5×10^4 6.1×10^2	0.345 0.208
0.050 (2)	7.2010 (1)	7.3682 (2)	295–557 557–754	1.1×10^4 1.6×10^3	0.332 0.241
0.055 (1)	7.2052 (1)	7.3716 (1)	294–427 427–623	5.5×10^4 3.0×10^3	0.371 0.265
0.080 (1)	7.2132 (1)	7.3802 (1)	295–419 419–531	9.0×10^4 6.3×10^3	0.389 0.294
0.086 (2)	7.2142 (2)	7.3806 (1)	294–436 436–614	1.2×10^5 2.7×10^3	0.397 0.257

The dependence lg $\sigma_{dc}(y)$ at room temperature for the solid electrolyte $La_{1-y}Ba_yF_{3-y}$, plotted based on our results and data [5,38], is shown in Figure 5b. In the range of compositions y = 0.006–0.086, the ionic conductivity varied from 1×10^{-5} to 8.5×10^{-5} S/cm.

The coordinates of the conductivity maximum were $\sigma_{max} = 8.5 \times 10^{-5}$ S/cm and $y_{max} = 0.05 \pm 0.01$. The minimum activation enthalpy ΔH_{σ} = 0.33 eV (low-temperature segment $\sigma_{dc}(T)$) corresponded to the maximum conducting composition y_{max}.

Note that the nonstoichiometric $R_{1-y}M_yF_{3-y}$ crystals with a tysonite-type structure have an advantage in conductivity value over crystals with a fluorite-type structure $M_{1-x}R_xF_{2+x}$ [3]. Apparently, this is due to the features of defect formation in these two structures. The conductivity is equalized in value only when the fluorite-type crystals are heated to 150–200 °C, which significantly complicates their practical application.

The coordinates of the conductivity maxima (y_{max}, σ_{max}) for a large family of tysonite-type solid electrolytes $R_{1-y}M_yF_{3-y}$ with M = Ca, Sr, Ba, Pb, Eu^{2+} and R = La, Ce, Pr, Nd are presented in Table 2. It can be seen that the maxima of ionic conductivity were realized in a narrow concentration range of y = 0.03–0.05. This fact indicates a weak effect of the R^{3+} and M^{2+}cations sizes on the value of the coordinate y_{max} for this type of solid electrolytes with heterovalent isomorphic substitutions.

Table 2. Coordinates of the maxima (y_{max}, σ_{max}) on the dependences $\sigma_{dc}(y)$ at room temperature for $R_{1-y}M_yF_{3-y}$ solid electrolytes.

Composition	Material Type *	y_{max}	$\sigma_{\mu\alpha\xi}$, Σ/Aμ	Reference
$La_{1-y}Ba_yF_{3-y}$	S	0.05 ± 0.01	8.5×10^{-5}	This work
	—«—	0.05	8×10^{-5}	[39]
	—«—	0.07–0.09	8×10^{-5}	[5]
	P	0.04	3×10^{-5}	[21]
	—«—	0.05	2×10^{-5}	[24]
	—«—	0.05	4×10^{-5}	[40]
	—«—	0.06	6×10^{-5}	[16]
	—«—	0.05—0.07	6×10^{-5}	[22]
$La_{1-y}Sr_yF_{3-y}$	S	0.05	2×10^{-4}	[41]
	—«—	0.03	3×10^{-4}	[42]
	P	0.05	5×10^{-5}	[21]
$La_{1-y}Ca_yF_{3-y}$	P	0.06	8×10^{-6}	[21]
$Ce_{1-y}Ba_yF_{3-y}$	P	0.05	1×10^{-4}	[43]
	—«—	0.04–0.06	–	[44]
$Ce_{1-y}Sr_yF_{3-y}$	S	0.03	5×10^{-4}	[45]
	P	0.04	1×10^{-4}	[44]
	—«—	0.07	3×10^{-5}	[43]
	—«—	0.06	8×10^{-5}	[16]
$Ce_{1-y}Ca_yF_{3-y}$	P	0.05	2×10^{-4}	[43]
	—«—	0.04–0.06	–	[44]
$Pr_{1-y}Sr_yF_{3-y}$	S	0.03	5×10^{-4}	[45]
$Pr_{1-y}Pb_yF_{3-y}$	S	0.04	7×10^{-5}	[46]
$Nd_{1-y}Ba_yF_{3-y}$	P	0.04–0.05	–	[47]
$Nd_{1-y}Sr_yF_{3-y}$	S	0.03	3×10^{-4}	[45]
	P	0.04–0.05	–	[47]
$Nd_{1-y}Ca_yF_{3-y}$	S	0.05	1.5×10^{-4}	[48]
	P	0.04–0.05	–	[47]
$Nd_{1-y}Eu_yF_{3-y}$	S	0.03	2×10^{-4}	[49]
$Nd_{1-y}Pb_yF_{3-y}$	S	0.05	3×10^{-5}	[46]

* S—single crystals, P—polycrystals.

4. Conclusions

The series of $La_{1-y}Ba_yF_{3-y}$ solid electrolyte crystals with $0.00 \leq y \leq 0.12$ was successfully grown from the melt by the Bridgman technique. Temperature measurements of the ionic conductivity of $La_{1-y}Ba_yF_{3-y}$ crystals by impedance spectroscopy were carried out in the range of 294 to 800 K. The composition of single-crystal samples was refined in terms of the unit cell parameters and density for the $La_{1-y}Ba_yF_{3-y}$ tysonite-type phase. The results of conductometric data for $La_{1-y}Ba_yF_{3-y}$ single crystals indicate that the $\sigma_{dc}(y)$ dependence had a maximum $\sigma_{max} = 8.5 \times 10^{-5}$ S/cm at $y_{max} = 0.05 \pm 0.01$. Analysis of the published data on the compositions of the conductivity maxima for a large family of solid electrolytes $R_{1-y}M_yF_{3-y}$ (M = Ca, Sr, Ba, Eu^{2+} and R = La, Ce, Pr, Nd) showed that they fall within the range of $0.03 \leq y_{max} \leq 0.05$ regardless of the type of R^{3+} and M^{2+} cations. It is shown that the size of the cation forming a solid solution practically does not affect the value of y_{max} for $R_{1-y}M_yF_{3-y}$ solid electrolytes.

Despite the high level of room temperature conductivity of the studied LaF_3-based materials, crystals of $R_{1-y}M_yF_{3-y}$ (R = Ce, Pr, Nd; M = Ca, Sr) should be considered promising for practical implementation as a solid electrolyte with better electrophysical characteristics. It is these crystals that will become the next step in solid-state ionics as

room temperature fluoride solid electrolytes and as promising polyfunctional crystalline materials of the future.

Author Contributions: D.N.K., I.I.B., N.I.S. performed the experiments, prepared figures, and manuscript; D.N.K., I.I.B. performed crystal growth experiments, analyzed the data, interpreted experiments; N.I.S. performed conductivity investigation; D.N.K. provided the idea, designed the experiments; D.N.K. coordinated the scientific group. All authors have read and agreed to the published version of the manuscript.

Funding: This research was supported by the Russian Foundation for Basic Research (project 19-02-00877) in the part concerning the growth of crystals and by the Ministry of Higher Education and Science of the Russian Federation within the State assignment of the Federal Scientific Research Centre "Crystallography and Photonics" of the Russian Academy of Sciences in the part concerning investigation and analysis of crystal properties using the equipment of the Shared Research Center (project RFMEFI62119X0035).

Data Availability Statement: Data sharing not applicable. (No new data were created or analyzed in this study. Data sharing is not applicable to this article).

Acknowledgments: We are grateful to N.A. Ivanovskaya, N.A. Arkharova, A.G. Ivanova, and A.G. Savelyev for their help in obtaining experimental data.

Conflicts of Interest: The authors declare no conflict of interest. The funders had no role in the design of the study; in the collection, analyses, or interpretation of data; in the writing of the manuscript, or in the decision to publish the results.

References

1. Sobolev, B.P.; Tkachenko, N.L. Phase diagrams of BaF_2-(Y, Ln)F_3 systems. *J. Less-Common Met.* **1982**, *85*, 155–170. [CrossRef]
2. Sylianova, E.A.; Karimov, D.N.; Sobolev, B.P. Displacements in the cationic motif of nonstoichiometric fluorite phases $Ba_{1-x}R_xF_{2+x}$ as a result of the formation of $\{Ba_8[R_6F_{68-69}]\}$ clusters: III. Defect cluster structure of the nonstoichiometric phase $Ba_{0.69}La_{0.31}F_{2.31}$ and its dependence on heat treatment. *Crystals* **2021**, *11*, 147. [CrossRef]
3. Sobolev, B.P.; Sorokin, N.I.; Bolotina, N.B. Nonstoichiometric single crystals $M_{1-x}R_xF_{2+x}$ and $R_{1-y}M_yF_{3-y}$ (*M*–Ca, Sr, Ba; *R*—rare earth elements) as fluorine-conducting solid electrolytes. In *Progress in Fluorine Science. Photonic & Electronic Properties of Fluoride, Materials*; Tressaud, A., Poeppelmeier, K., Eds.; Elsevier: Amsterdam, The Netherlands, 2016; Chapter 21; Volume 1, pp. 465–491. [CrossRef]
4. Wapenaar, K.E.D.; Van Koesveld, J.L.; Schoonman, J. Conductivity enhancement in fluorite-structured $Ba_{1-x}La_xF_{2+x}$ solid solutions. *Solid State Ion.* **1981**, *2*, 145–154. [CrossRef]
5. Roos, A.; Van de Pol, F.C.M.; Keim, R.; Schoonman, J. Ionic conductivity in tysonite-type solid solutions $La_{1-x}Ba_xF_{3-x}$. *Solid State Ion.* **1984**, *13*, 191–203. [CrossRef]
6. Ivanov-Shits, A.K.; Sorokin, N.I.; Fedorov, P.P.; Sobolev, B.P. Specific features of ion transport in non-stoichiometric fluorite-type $Ba_{1-x}R_xF_{2+x}$ (R = La − Lu) phases. *Solid State Ion.* **1989**, *31*, 269–280. [CrossRef]
7. Sorokin, N.I.; Breiter, M.W. Anionic conductivity and thermal stability of single crystals of solid solutions based on barium fluoride. *Solid State Ion.* **1997**, *99*, 241–250. [CrossRef]
8. Roos, A.; Schoonman, J. Electronic conductivity in $La_{1-x}Ba_xF_{3-x}$ crystals. *Solid State Ion.* **1984**, *13*, 205–211. [CrossRef]
9. Reddy, S.N.S.; Rapp, R.A. Electronic conduction in the BaF_2 solid electrolyte. *J. Electrochem. Soc.* **1979**, *126*, 2023–2025. [CrossRef]
10. Krivandina, E.A. Preparation of single crystals of multicomponent fluoride materials with the fluorite type structure. *Butll. Soc. Cat. Cien.* **1991**, *12*, 393–412. Available online: https://www.raco.cat/index.php/ButlletiSCFQMT/article/view/21735 (accessed on 13 May 2021).
11. Sobolev, B.P. *The Rare Earth Trifluorides, Part 1*; The High Temperature Chemistry of the Rare Earth Trifluorides, Institutd'Estudis Catalans: Barcelona, Spain, 2000; 520p, Available online: www.books.google.ru/books/rareearthtrifluorides (accessed on 13 May 2021).
12. Mohammad, I.; Witter, R.; Fichtner, M.; Reddy, M.A. Introducing interlayer electrolytes: Toward room-temperature high-potential solid-state rechargeable fluoride ion batteries. *ASC Appl. Energy Mater.* **2019**, *2*, 1553–1562. [CrossRef]
13. Gschwind, F.; Rodriquez-Garcia, G.; Sandbeck, D.J.S.; Gross, A.; Weil, M.; Fichtner, M.; Hörmannet, N. Fluoride ion batteries: Theoretical performance, safety, toxicity, and a combinatorial screening of new electrodes. *J. Fluor. Chem.* **2016**, *182*, 76–90. [CrossRef]
14. Liu, L.; Yang, L.; Liu, M.; Wang, X.; Li, X.; Shao, D.; Luo, K.; Luo, Z.; Chen, G. A flexible tysonite-type $La_{0.95}Ba_{0.05}F_{2.95}$@PEO-based composite electrolyte for the application of advanced fluoride ion battery. *J. Energy Storage* **2019**, *25*, 100886. [CrossRef]
15. Reddy, M.A.; Fichtner, M. Batteries based on fluoride shuttle. *J. Mater. Chem.* **2011**, *21*, 17059–17062. [CrossRef]
16. Potanin, A.A. Solid-state chemical current source based on an ionic conductor such as lanthanum trifluoride. *Russ. Chem. J.* **2001**, *45*, 61–66. Available online: http://www.chem.msu.su/rus/jvho/2001-5-6/58.pdf (accessed on 13 May 2021).

17. Krivandina, E.A.; Zhmurova, Z.I.; Sobolev, B.P.; Glushkova, T.M.; Kiselev, D.F.; Firsova, M.M.; Shtyrkova, A.P. Growth of $R_{1-y}Sr_yF_{3-y}$ crystals with rare earth elements of the cerium subgroup (R = La, Ce, Pr, or Nd; $0 \leq y \leq 0.16$) and the dependence of their density and optical characteristics on composition. *Crystallogr. Rep.* **2006**, *51*, 895–901. [CrossRef]
18. Roos, A. Crystal growth of solid solutions $La_{1-x}Ba_xF_{3-x}$. *Mater. Res. Bull.* **1983**, *18*, 405–409. [CrossRef]
19. Vasyliev, V.; Molina, P.; Nakamura, M.; Víllora, E.G.; Shimamura, K. Magneto-optical properties of $Tb_{0.81}Ca_{0.19}F_{2.81}$ and $Tb_{0.76}Sr_{0.24}F_{2.76}$ single crystals. *Opt. Mater.* **2011**, *33*, 1710. [CrossRef]
20. Ananyeva, G.V.; Baranova, E.N.; Zarzhitskaya, M.N.; Ivanova, I.A.; Koryakina, L.F.; Petrova, M.A.; Podkolzina, I.G.; Semenova, T.S.; Yagmurova, G.P. Growth and physicochemical study of single crystals of tysonite solid solutions $(Y, Ln)_{1-x}Sr_xF_{3-x}$. *Izv. Akad. Nauk SSSR Ser. Neorg. Mater.* **1980**, *16*, 68–72. (In Russian)
21. Murin, I.V.; Glumov, O.V.; Amelin, Y.V. Ion transfer mechanism in LaF_3. *J. Appl. Chem. USSR* **1980**, *53*, 1474–1478.
22. Chable, J.; Dieudonné, B.; Body, M.; Legein, C.; Crosnier-Lopez, M.-P.; Galven, C.; Mauvy, F.; Durand, E.; Fourcade, S.; Sheptyakov, D.; et al. Fluoride solid electrolytes: Investigation of the tysonite-type solid solutions $La_{1-x}Ba_xF_{3-x}$ (x <0.15). *Dalton Trans.* **2015**, *44*, 19625–19635. [CrossRef]
23. Motohashi, K.; Nakamura, T.; Kimura, Y.; Uchimoto, Y.; Amezawa, K. Influence of microstructures on conductivity in tysonite-type fluoride ion conductors. *Solid State Ion.* **2019**, *338*, 113–120. [CrossRef]
24. Bhatia, H.; Thieu, D.T.; Pohl, A.H.; Chakravadhanula, V.S.K.; Fawey, M.H.; Kübel, C.; Fichtner, M. Conductivity optimization of tysonite-type $La_{1-x}Ba_xF_{3-x}$ solid electrolytes for advanced fluoride ion battery. *ACS Appl. Mater. Interfaces* **2017**, *9*, 23707–23715. [CrossRef] [PubMed]
25. Rongeat, C.; Reddy, M.A.; Witter, R.; Fichtner, M. Solid electrolytes for fluoride ion batteries: Ionic conductivity in polycrystalline tysonite-type fluorides. *ARS Appl. Mater. Interfaces* **2014**, *6*, 2103–2110. [CrossRef]
26. Duvel, A.; Bednarcik, J.; Sepelak, V.; Heitjans, P. Mechanosynthesis of the Fast fluoride ion conductor $Ba_{1-x}La_xF_{2+x}$: From the fluorite to the tysonite Structure. *J. Phys. Chem. C* **2014**, *118*, 7117–7129. [CrossRef]
27. Breuer, S.; Gombotz, M.; Pregartner, V.; Hanzu, I.; Wilkening, M. Heterogeneous F anion transport, local dynamics and electrochemical stability of nanocrystalline $La_{1-x}Ba_xF_{3-x}$. *Energy Storage Mater.* **2019**, *16*, 481–490. [CrossRef]
28. Chable, J.; Martin, A.G.; Bourdin, A.; Body, M.; Legein, C.; Jouanneaux, A.; Crosnier-Lopez, M.-P.; Galven, C.; Dieudonné, B.; Leblanc, M.; et al. Fluoride solid electrolytes: From microcrystalline to nanostructured tysonite-type $La_{0.95}Ba_{0.05}F_{2.95}$. *J. Alloys Compd.* **2017**, *692*, 980–988. [CrossRef]
29. Gombolz, M.; Pregartner, V.; Hanzu, I.; Wilkening, H.M.R. Fluoride-ion batteries: On the electrochemical stability of nanocrystalline $La_{0.9}Ba_{0.1}F_{2.9}$ against metal electrodes. *Nanomaterials* **2019**, *9*, 1517. [CrossRef]
30. Zhang, L.; Reddy, A.M.; Fichtner, M. Development of tysonite-type fluoride conducting thin film electrolytes for fluoride ion batteries. *Solid State Ion.* **2015**, *272*, 39–44. [CrossRef]
31. Toma, O.; Rotella, H.; Dahab, H.; Maisonneuve, V.; Boulard, B. Tysonite-type solid state electrolyte for fluoride ion batteries: Highly dense thin film by PVD processing. *J. Alloys Compd.* **2021**, *862*, 158683. [CrossRef]
32. Krivandina, E.A.; Zhmurova, Z.I.; Glushkova, T.M.; Firsova, M.M.; Shtyrkova, A.P.; Sobolev, B.P. Congruently melting compositions in the series of solid solutions $R_{1-x}Sr_xF_{3-x}$ (R = La–Nd, $0 \leq x \leq 0.15$) with tysonite structure (Refinement by directional crystallization). *Crystallogr. Rep.* **2003**, *48*, 878–882. [CrossRef]
33. Krivandina, E.A.; Zhmurova, Z.I.; Berezhkova, G.V.; Sobolev, B.P.; Glushkova, T.M.; Kiselev, D.F.; Firsova, M.M.; Shtyrkova, A.P. Crystal growth, density, and mechanical properties of $La_{1-x}Sr_xF_{3-x}$ solid solutions (0 <x <0.15) with the tysonite structure. *Crystallogr. Rep.* **1995**, *40*, 686–690.
34. Buchinskaya, I.I.; Arkharova, N.A.; Ivanova, A.G.; Karimov, D.N. Growth of crystals of solid solutions with tysonite structure in the PbF_2–RF_3 systems (R = Pr, Nd). *Crystallogr. Rep.* **2020**, *65*, 147–151. [CrossRef]
35. Sorokin, N.I.; Krivandina, E.A.; Zhmurova, Z.I. Dependences of the density of $M_{1-x}R_xF_{2+x}$ and $R_{1-y}M_yF_{3-y}$ single crystals (M = Ca, Sr, Ba, Cd, Pb; R means rare earth elements) on composition. *Crystallogr. Rep.* **2013**, *58*, 948–952. [CrossRef]
36. Ivanov-Shits, A.K.; Sorokin, N.I.; Fedorov, P.P.; Sobolev, B.P. Conductivity of $Sr_{1-x}La_xF_{2+x}$ solid solutions. *Soviet Phys. Solid State* **1983**, *25*, 1007–1010.
37. Chernaya, T.S.; Verin, I.A.; Khrykina, O.N.; Bolotina, N.B. Defect Structures of $La_{1-y}Sr_yF_{3-y}$, $La_{1-y}Ba_yF_{3-y}$, and $Nd_{1-y}Ca_yF_{3-y}$ (y = 0.05, 0.10) nonstoichiometric tysonite phases. *Crystallogr. Rep.* **2018**, *63*, 45–51. [CrossRef]
38. Sorokin, N.I.; Sobolev, B.P.; Krivandina, E.A.; Zhmurova, Z.I. Optimization of single crystals of solid electrolytes with tysonite-type structure (LaF_3) for conductivity at 293 K: 2. Nonstoichiometric phases $R_{1-y}M_yF_{3-y}$(R = La-Lu, Y.; M = Sr, Ba). *Crystallogr. Rep.* **2015**, *60*, 123–129. [CrossRef]
39. Sorokin, N.I.; Krivandina, E.A.; Zhmurova, Z.I.; Sobolev, B.P.; Fistul', V.V. Superionic conductivity of the heterovalent solid solutions $R_{1-x}M_xF_{3-x}$ (R = REE, M = Ca, Ba) with tysonite-type structure. *Phys. Solid State* **1999**, *41*, 573–575. [CrossRef]
40. Schoonman, J.; Oversluizen, G.; Wapenaar, K.E.D. Solid electrolyte properties of LaF_3. *Solid State Ion.* **1980**, *1*, 211–221. [CrossRef]
41. Sorokin, N.I.; Sobolev, B.P. The conductivity of single crystals $La_{1-x}Sr_xF_{3-x}$ ($0 \leqslant x \leqslant 0.15$) with tysonite structure. *Crystallogr. Rep.* **1994**, *39*, 810–814.
42. Geiger, H.; Schon, G.; Strok, H. Ionic conductivity of single crystals of the non-stoichiometric tysonite phase $La_{(1-x)}Sr_xF_{(3-x)}$ ($0 \leqslant x \leqslant 0.14$). *Solid State Ion.* **1985**, *15*, 155–158. [CrossRef]
43. Takahashi, T.; Iwahara, H.; Ishikawa, T. Ionic conductivity of doped cerium trifluoride. *J. Electrochem. Soc.* **1977**, *124*, 280–284. [CrossRef]

44. Murin, I.V.; Glumov, O.V.; Sobolev, B.P. Electrical conductivity of solid electrolytes based on CeF_3. *Vestnik LGU* **1980**, *10*, 84–88. (In Russian)
45. Sorokin, N.I.; Fominykh, M.V.; Krivandina, E.A.; Zhmurova, Z.I.; Sobolev, B.P. Ion transport in $R_{1-x}Sr_xF_{3-x}$ (R = La–Yb, Y) solid solutions with a LaF_3 (tysonite) structure. *Crystallogr. Rep.* **1996**, *41*, 292–301.
46. Sorokin, N.I.; Karimov, D.N.; Buchinskaya, I.I. Conductivity of $R_{1-y}Pb_yF_{3-y}$ (R = Pr, Nd) solid electrolytes with tysonite structure. *Russ. J. Electrochem.* **2021**, *57*, 1–8. (In Russian) [CrossRef]
47. Murin, I.V.; Glumov, O.V.; Glumov, A.V. Ion and electron transfer processes in solid electrolytes based on NdF_3. In Proceedings of the 7th All-Union Symposium on the Chemistry of Inorganic Fluorides, Nauka, Moscow, 9–12 October 1984; p. 232. (In Russian).
48. Sobolev, B.P.; Sorokin, N.I.; Krivandina, E.A.; Zhmurova, Z.I. 293-K-conductivity optimization for single crystals of solid electrolytes with tysonite structure (LaF_3): I. Nonstoichiometric phases $R_{1-y}Ca_yF_{3-y}$ (R = La-Lu, Y). *Crystallogr. Rep.* **2014**, *59*, 550–562. [CrossRef]
49. Karimov, D.N.; Sorokin, N.I.; Sobolev, B.P.; Sokolov, V.I. Growth of $Nd_{1-y}Eu_y^{2+}F_{3-y}$ single crystals with tysonite-type (LaF_3) structure and investigation of the concentration dependence of some their properties. *Crystallogr. Rep.* **2019**, *64*, 354–359. [CrossRef]